






Acute Hepatopancreatic Necrosis Disease-Causing *Vibrio parahaemolyticus* Strains Maintain an Antibacterial Type VI Secretion System with Versatile Effector Repertoires

Peng Li,^a Lisa N. Kinch,^b Ann Ray,^{a,b} Ankur B. Dalia,^{e,f,g}  Qian Cong,^{c,d} Linda M. Nunan,^h Andrew Camilli,^{e,f} Nick V. Grishin,^{b,c,d}  Dor Salomon,^{a,i}  Kim Orth^{a,b,c}

Department of Molecular Biology, University of Texas Southwestern Medical Center, Dallas, Texas, USA^a; Howard Hughes Medical Institute, University of Texas Southwestern Medical Center, Dallas, Texas, USA^b; Department of Biochemistry, University of Texas Southwestern Medical Center, Dallas, Texas, USA^c; Department of Biophysics, University of Texas Southwestern Medical Center, Dallas, Texas, USA^d; Department of Molecular Biology & Microbiology, Tufts University School of Medicine, Boston, Massachusetts, USA^e; Howard Hughes Medical Institute, Tufts University School of Medicine, Boston, Massachusetts, USA^f; Department of Biology, Indiana University, Bloomington, Indiana, USA^g; School of Animal & Comparative Biomedical Sciences, University of Arizona, Tucson, Arizona, USA^h; Department of Clinical Microbiology and Immunology, Sackler Faculty of Medicine, Tel Aviv University, Tel Aviv, Israelⁱ

ABSTRACT Acute hepatopancreatic necrosis disease (AHPND) is a newly emerging shrimp disease that has severely damaged the global shrimp industry. AHPND is caused by toxic strains of *Vibrio parahaemolyticus* that have acquired a “selfish plasmid” encoding the deadly binary toxins PirA^{VP}/PirB^{VP}. To better understand the repertoire of virulence factors in AHPND-causing *V. parahaemolyticus*, we conducted a comparative analysis using the genome sequences of the clinical strain RIMD2210633 and of environmental non-AHPND and toxic AHPND isolates of *V. parahaemolyticus*. Interestingly, we found that all of the AHPND strains, but none of the non-AHPND strains, harbor the antibacterial type VI secretion system 1 (T6SS1), which we previously identified and characterized in the clinical isolate RIMD2210633. This finding suggests that the acquisition of this T6SS might confer to AHPND-causing *V. parahaemolyticus* a fitness advantage over competing bacteria and facilitate shrimp infection. Additionally, we found highly dynamic effector loci in the T6SS1 of AHPND-causing strains, leading to diverse effector repertoires. Our discovery provides novel insights into AHPND-causing pathogens and reveals a potential target for disease control.

IMPORTANCE Acute hepatopancreatic necrosis disease (AHPND) is a serious disease that has caused severe damage and significant financial losses to the global shrimp industry. To better understand and prevent this shrimp disease, it is essential to thoroughly characterize its causative agent, *Vibrio parahaemolyticus*. Although the plasmid-encoded binary toxins PirA^{VP}/PirB^{VP} have been shown to be the primary cause of AHPND, it remains unknown whether other virulent factors are commonly present in *V. parahaemolyticus* and might play important roles during shrimp infection. Here, we analyzed the genome sequences of clinical, non-AHPND, and AHPND strains to characterize their repertoires of key virulence determinants. Our studies reveal that an antibacterial type VI secretion system is associated with the AHPND strains and differentiates them from non-AHPND strains, similar to what was seen with the PirA/PirB toxins. We propose that T6SS1 provides a selective advantage during shrimp infections.

Received 30 March 2017 Accepted 18 April 2017

Accepted manuscript posted online 21 April 2017

Citation Li P, Kinch LN, Ray A, Dalia AB, Cong Q, Nunan LM, Camilli A, Grishin NV, Salomon D, Orth K. 2017. Acute hepatopancreatic necrosis disease-causing *Vibrio parahaemolyticus* strains maintain an antibacterial type VI secretion system with versatile effector repertoires. *Appl Environ Microbiol* 83:e00737-17. <https://doi.org/10.1128/AEM.00737-17>.

Editor Eric V. Stabb, University of Georgia

Copyright © 2017 American Society for Microbiology. All Rights Reserved.

Address correspondence to Dor Salomon, dorsalomon@mail.tau.ac.il, or Kim Orth, kim.orth@utsouthwestern.edu.

KEYWORDS AHPND, T3SS, T6SS, *Vibrio*, *Vibrio parahaemolyticus*, shrimp, type III secretion system, type VI secretion system, MIX effectors

Acute hepatopancreatic necrosis disease (AHPND), previously named early mortality syndrome (EMS), is a newly emerging shrimp disease that is causing serious reductions in shrimp production and financial losses to the global shrimp aquaculture industry (1, 2). Since the disease outbreak first appeared in China in 2009, it quickly spread to Vietnam in 2010, Malaysia in 2011, Thailand in 2012, Mexico in 2013, the Philippines in 2015, and South America in 2016 (1, 3–6). AHPND can cause up to 100% mortality within about 20 to 30 days after a pond gets stocked with shrimp postlarvae (7). Notable symptoms of affected shrimp include an empty gut and an atrophied, pale hepatopancreas (2). Histopathology analysis shows sloughing of the hepatopancreatic tubule epithelial cells and hemocytic infiltration (1). In 2013, it was discovered that AHPND was caused by a specific set of *Vibrio parahaemolyticus* strains (1). Toxic AHPND-causing *V. parahaemolyticus* strains acquired a 63- to 70-kb plasmid encoding the binary toxins PirA^{VP}/PirB^{VP}, which are homologous to the *Photobacterium luminescens* insect-related (Pir) toxins PirA/PirB (8, 9). PirA^{VP}/PirB^{VP} are secreted toxins that were determined to be the primary virulence factors causing AHPND (8, 9). Based on their structure, these toxins are similar to Cry insecticidal toxin-like proteins that encode a pore-forming activity used to kill host cells (8). This plasmid also encodes a set of conjugative transfer and mobilization genes that could facilitate its spread between different *Vibrio* species (8). It is also interesting that this is a “selfish plasmid” that contains a *pndA* toxin/antitoxin system ensuring the acquisition of this plasmid in bacterial progeny for survival (8).

In 2015, a strain of *Vibrio campbellii* isolated from Vietnam and a strain of *Vibrio owensii* isolated from China were shown to cause AHPND (10–12). Both strains contain a plasmid that is highly similar to the one discovered in AHPND-causing *V. parahaemolyticus* and encodes the binary toxins homologous to PirA/PirB (10–12). It supports the model that PirA^{VP}/PirB^{VP} are the main virulence factors causing AHPND. This discovery is also consistent with the hypothesis that this plasmid is transmissible and may be shared between different *Vibrio* species (8, 12).

V. parahaemolyticus is a Gram-negative, halophilic bacterium that naturally lives in warm marine and estuarine environments found throughout the world (13, 14). Rising ocean temperatures during recent years have contributed to its global dissemination (15–20). *V. parahaemolyticus* is the world’s leading cause of acute gastroenteritis due to the consumption of raw or undercooked seafood (18). It can also cause infection of open wounds through the exposure to contaminated warm seawater (19). In immunocompetent individuals, *V. parahaemolyticus* infection is normally self-limiting and lasts for about 2 to 3 days (18, 19), but for individuals with underlying health conditions, the infection can lead to severe diarrhea, septicemia, and in some cases subsequent death (18, 19).

Despite the discovery of the toxic plasmid and binary toxins PirA^{VP}/PirB^{VP}, no comprehensive studies have been done to characterize the other important virulence determinants commonly found in *V. parahaemolyticus*, such as thermostable direct hemolysin (TDH) and TDH-related hemolysin (TRH) toxins, two type III secretion systems (T3SSs) and two type VI secretion systems (T6SSs) (21). TDH and TRH are pore-forming toxins with hemolytic activities (13). T3SS is a conserved secretory system present in many Gram-negative bacteria that directly delivers bacterial virulence factors, called effectors, into the cytoplasm of host cells to exert various functions (22). *V. parahaemolyticus* can contain two different T3SSs (T3SS1 and T3SS2) (13, 23). T3SS1 is highly conserved and present in both environmental and clinical isolates of *V. parahaemolyticus* (24). It is activated by low-Ca²⁺ environments as mimicked by the serum-free Dulbecco’s modified Eagle medium (DMEM) and possesses cytotoxicity against various cultured eukaryotic cell lines (25, 26). In contrast, T3SS2 is found only in clinical isolates of *V. parahaemolyticus* (24). It is activated by bile salts and is the primary virulence factor

for gastroenteritis during human infection (27–30). T6SS is another protein secretion apparatus present in various Gram-negative bacteria (31). Increasing evidence suggests that the majority of T6SSs play a role in interbacterial competition, as they possess antibacterial activities mediated by delivery of toxic effectors into neighboring cells (31–33). Importantly, bacteria avoid self-intoxication by these T6SSs with encoded immunity proteins that protect against cognate antibacterial effectors. These T6SS effector/immunity (E/I) pairs are encoded as bicistronic units (34, 35). Two T6SSs have been described in *V. parahaemolyticus*, T6SS1 and T6SS2 (36). T6SS1 has previously been associated predominantly with clinical isolates of *V. parahaemolyticus* and was shown to possess antibacterial activities against various bacterial competitors (36–38). In the clinical isolate RIMD2210633, this antibacterial activity is mediated by at least three delivered toxins, two of which contain an N-terminal MIX (Marker for type sIX effector) domain and are therefore members of the T6SS MIX effector class (35). T6SS2, like T3SS1, is present in all *V. parahaemolyticus* strains, including both environmental and clinical strains (36, 37), but its role in the *V. parahaemolyticus* life cycle remains unknown. The two *V. parahaemolyticus* T6SSs are differentially regulated by external cues such as temperature, salinity, and surface sensing (36).

To better understand the genetic features of AHPND-causing *V. parahaemolyticus*, we selected a set of 18 isolates of *V. parahaemolyticus*, including 5 environmental non-AHPND isolates, 12 toxic AHPND isolates, and 1 clinical isolate. The clinical isolate, RIMD2210633, is not associated with the shrimp disease but rather with gastroenteritis observed in a human host (39). Comparative analysis was conducted using the genome sequences of these strains to provide novel insights about their key virulence determinants. Our studies showed that all of the 12 AHPND *V. parahaemolyticus* strains possess the same binary toxins PirA^{VP}/PirB^{VP}, suggesting that these toxins likely share the same origin (12). All *V. parahaemolyticus* strains analyzed in this study contain the highly conserved T3SS1 and T6SS2. None of these strains encode T3SS2 and TDH/TRH toxin, except for the clinical isolate RIMD2210633; T3SS2 and TDH/TRH are associated with incidence of gastroenteritis. Interestingly, all toxic AHPND isolates possess an antibacterial T6SS1 similar to the one found in the clinical isolate RIMD2210633, suggesting a possible role of the T6SS1 in facilitating shrimp infection by killing competitor bacteria and conferring to pathogenic AHPND *V. parahaemolyticus* a fitness advantage (36).

RESULTS

***Vibrio parahaemolyticus* clinical, environmental non-AHPND, and toxic AHPND strains contain different virulence factors.** Genome sequences of 1 clinical, 5 environmental non-AHPND, and 12 toxic AHPND strains of *V. parahaemolyticus* were collected for comparative genome analysis (for a list of strains, see Table 1). Among these, we generated draft genomes of four strains, including one non-AHPND strain (A2) and three AHPND strains (1335, 12297B, and D4). The genome sequence data for the other strains were obtained from the NCBI database. RIMD2210633 is a clinical isolate that served as a reference strain, and the other strains were isolated from various countries affected by AHPND, including China (CN), Vietnam (VT), Thailand (TH), and Mexico (MX). We searched the genomes of all these *V. parahaemolyticus* strains for known key virulence factors, such as the binary toxins PirA^{VP}/PirB^{VP}, T3SSs (T3SS1 and T3SS2), TDH/TRH toxins, and T6SSs (T6SS1 and T6SS2). The analysis results are summarized in Table 1. Remarkably, two features clearly distinguished the AHPND from the non-AHPND *V. parahaemolyticus* strains. As expected, the virulent PirA^{VP}/PirB^{VP} toxins were found only in the AHPND-causing strains. In addition, T6SS1, associated predominantly with clinical isolates in previous studies, was present in all AHPND-causing strains but in none of the non-AHPND environmental strains (Table 1).

Binary toxins PirA^{VP}/PirB^{VP}. A comparison of the binary toxins PirA^{VP}/PirB^{VP} from different AHPND strains of *V. parahaemolyticus* showed that they have identical protein sequences, suggesting that all of the PirA^{VP}/PirB^{VP} toxins very likely have the same origin. Strain FIM-S1708+ was excluded from this analysis because the genome se-

TABLE 1 Summary of toxins and virulence determinants in different *V. parahaemolyticus* strains analyzed in this study

Strain type	Origin ^a	Strain name	PirA ^{VP} / PirB ^{VP}	T3SS1	T3SS2	TDH/ TRH	T6SS1	T6SS2	Yr isolated ^b	Associated with disease	Accession number(s)	Reference or source
Clinical	JP	RIMD2210633	–	+	+	+	+	+	1996	+	NC_004603 , NC_004605	61
Non-AHPND	VT	A2	–	+	–	–	–	+	2013	–	MWVH000000000	This study
	TH	TUMSAT_H01_S4	–	+	–	–	–	+	2014	–	BAV100000000	62
		TUMSAT_H10_S6	–	+	–	–	–	+	2014	–	BAVK000000000	62
		NCKU_TN_S02	–	+	–	–	–	+	2014	–	JPKV000000000	63
	MX	FIM-S1392–	–	+	–	–	–	+	2014	–	JPLU000000000	64
AHPND	VT	A3	+	+	–	–	+	+	2014	+	NZ_JOKE000000000	65
		1335	+	+	–	–	+	+	2013	+	MYFF000000000	This study
		12297B	+	+	–	–	+	+	2013	+	MYFG000000000	This study
	TH	TUMSAT_DE1_S1	+	+	–	–	+	+	2014	+	BAVF000000000	62
		TUMSAT_DE2_S2	+	+	–	–	+	+	2014	+	BAVG000000000	62
		TUMSAT_D06_S3	+	+	–	–	+	+	2014	+	BAVH000000000	62
		NCKU_TV_3HP	+	+	–	–	+	+	2014	+	JPKS000000000	63
		NCKU_TV_5HP	+	+	–	–	+	+	2014	+	JPKT000000000	62
	CN	NCKU_CV_CHN	+	+	–	–	+	+	2014	+	JPKU000000000	63
		D4	+	+	–	–	+	+	2013	+	MYFH000000000	This study
	MX	M0605	+	+	–	–	+	+	2013	+	JALL000000000	4
		FIM-S1708+	+	+	–	–	+	+	2014	+	JPLV000000000	64

^aJP, Japan; VT, Vietnam; TH, Thailand; MX, Mexico; CN, China.

^bAs best can be inferred from references.

quence of this isolate did not contain complete *pirA^{VP}* and *pirB^{VP}* genes. The *pirA^{VP}* and *pirB^{VP}* genes are flanked by two inverted copies of a transposase, suggesting that the toxic genes are likely acquired by AHPND strains from an unknown foreign source (8, 12). PirA^{VP}/PirB^{VP} are homologues of the insecticidal toxins PirA/PirB of the *Photorhabdus* and *Xenorhabdus* genera (8). Although the mechanism underlying the toxicity of PirA^{VP}/PirB^{VP} is still unknown, the binary toxins share high structural similarities with the *Bacillus* pore-forming Cry insecticidal toxin (8).

T3SS and TDH/TRH toxins. *V. parahaemolyticus* possesses two different T3SSs, called T3SS1 and T3SS2 (13, 23). T3SS1 is present in all sequenced strains of *V. parahaemolyticus*, including both environmental and clinical isolates (24). The T3SS1 pathogenicity island contains 49 genes, with the main cluster (*vp1656-vp1702*) located on chromosome 1 and two genes (*vpa0450* and *vpa0451*) on chromosome 2 (Fig. 1A) (13). All of the *V. parahaemolyticus* strains analyzed in our study contain this highly conserved T3SS1. Our analysis revealed a novel feature of T3SS1, namely, that there are two different subtypes of T3SS1, which we termed T3SS1a and T3SS1b (Fig. 1A). The clinical RIMD2210633 strain, all 5 non-AHPND strains, and 7 of the 12 AHPND strains have T3SS1a that contains *vp1676* to *vp1679* (Fig. 1A; shown in blue). The other five AHPND strains possess T3SS1b that contains three hypothetical genes at the locus corresponding to *vp1676-vp1679* of T3SS1a (Fig. 1A; shown in green). The functions of VP1676 to VP1679, as well as those of their counterparts in T3SS1b, remain unknown. VP1676 is a putative LysR family transcriptional regulator. VP1678 is a putative diene-lactone hydrolase. VP1677 and VP1679 are both annotated as hypothetical proteins. The three newly identified proteins in T3SS1b are annotated as a putative transcriptional regulator, a putative major facilitator superfamily (MFS) transporter, and a putative multidrug transporter, respectively.

T3SS1 contains four characterized effectors, VopQ (VP1680), VopR (VP1683), VopS (VP1686), and VPA0450, which orchestrate rapid cell death against multiple eukaryotic cell lines (13, 14). To test whether the T3SS1 of the *V. parahaemolyticus* strains analyzed in this study is functional, one non-AHPND strain and four AHPND strains as well as control strains derived from RIMD2210633 (POR1, POR2, and POR3) were used to infect HeLa cells (29). POR1 is referred to here as the parental strain; it is a derivative of the clinical isolate RIMD2210633 that encodes deletions for the two hemolysins (encoded by *tdh* and *trh*) (40). Using POR1 as the parental strain, POR2 had the *vcrD1* gene

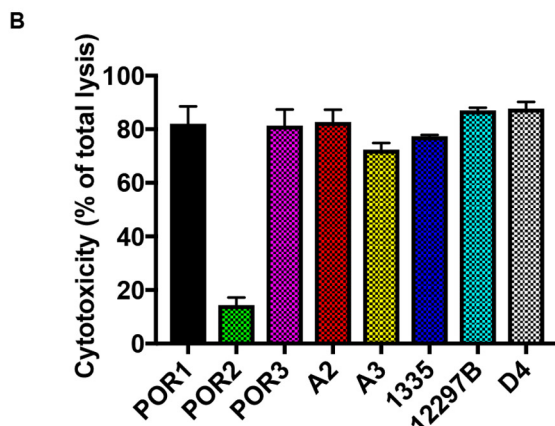
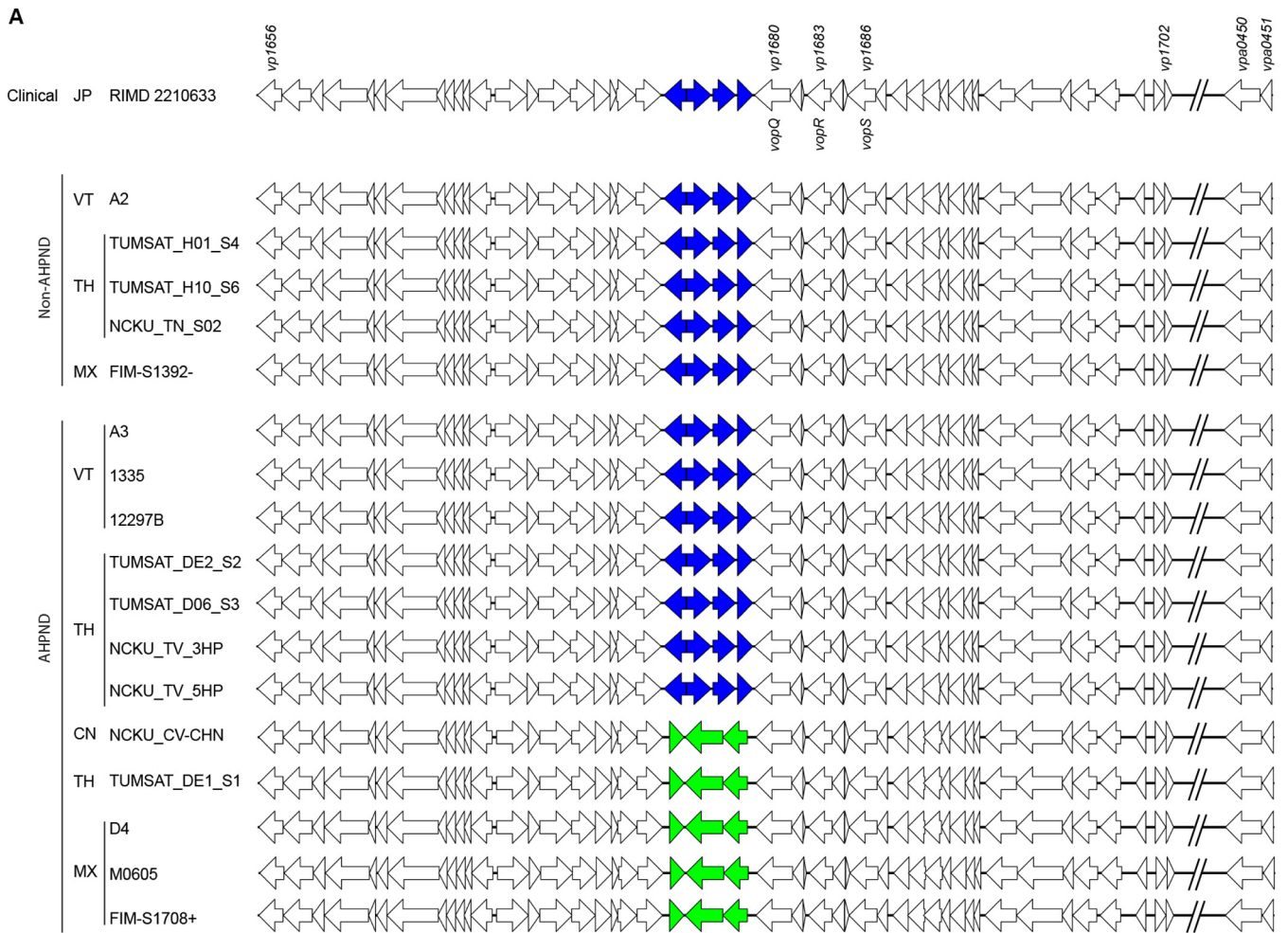


FIG 1 *V. parahaemolyticus* clinical, non-AHPND, and AHPND strains contain a conserved T3SS1. (A) Comparison of T3SS1 clusters from clinical, non-AHPND, and AHPND strains of *V. parahaemolyticus*. All *V. parahaemolyticus* strains analyzed in this study contain a highly conserved T3SS1 that is further categorized into two subtypes, T3SS1a and T3SS1b. T3SS1a contains *vp1676* to *vp1679* (blue), and T3SS1b contains three newly identified genes (green). JP, Japan; VT, Vietnam; TH, Thailand; MX, Mexico; CN, China. (B) HeLa cells were infected with the indicated *V. parahaemolyticus* strains for 4 h at an MOI of 10. Lactate dehydrogenase (LDH) release was evaluated as the measure of cytotoxicity against host cells. Data are means \pm standard deviations (SD); $n = 3$. Data are representative of three independent experiments.

deleted to inactivate T3SS1, and POR3 had the *vcrD2* gene deleted to inactivate T3SS2 (29, 40). Their cytotoxicity was evaluated at 4 h postinfection by measuring the release of lactate dehydrogenase (LDH) into the culture medium during cell death. As expected, all the strains containing T3SS1 exhibited similar cytotoxicity toward HeLa cells,

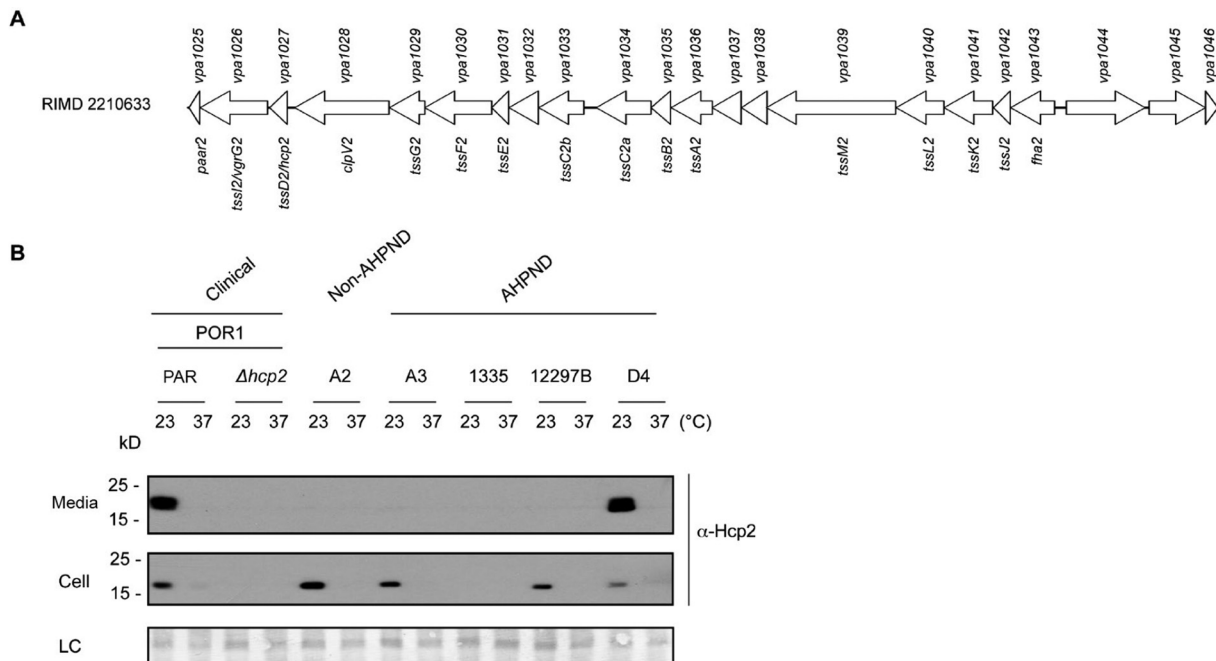


FIG 2 *V. parahaemolyticus* clinical, non-AHPND, and AHPND strains contain a conserved but differentially regulated T6SS2. (A) Schematic representation of the *V. parahaemolyticus* T6SS2 gene cluster. RIMD2210633 strain locus numbers are shown above and gene names below. (B) Expression (Cell) and secretion (Media) of *V. parahaemolyticus* T6SS2 component Hcp2 by the indicated *V. parahaemolyticus* strains grown in LB at 23°C or 37°C for 5 h and analyzed by Western blotting using α -Hcp2 antibody. PAR, parental strain. LC, loading control.

which suggests that their T3SS1 is active (Fig. 1B). The control POR2 strain, in which T3SS1 is inactive, was unable to kill HeLa cells (Fig. 1B).

None of the *V. parahaemolyticus* strains that we analyzed, except for RIMD2210633, contains T3SS2, consistent with previous reports that this system is associated with clinical isolates of *V. parahaemolyticus* only (4). Therefore, it is unlikely that the AHPND *V. parahaemolyticus* strains identified so far could infect human beings and cause gastroenteritis. TDH/TRH toxins are generally associated and encoded along with T3SS2 (24). Consistent with this association, all of the *V. parahaemolyticus* strains analyzed, other than RIMD2210633, also lacked the TDH/TRH toxins.

T6SS2. T6SS2 is highly conserved, located on chromosome 2, and found in all sequenced isolates of *V. parahaemolyticus* (36–38). The RIMD2210633 T6SS2 cluster contains 22 genes (locus tags *vpa1025* to *vpa1046*) (Fig. 2A). Consistent with previous discoveries, all of the *V. parahaemolyticus* strains analyzed in this study possess this conserved T6SS2 (Table 1). T6SS2 in RIMD2210633 is most active under low-salt (1% NaCl) conditions at 23°C and exhibits no activity at 37°C (36). To test whether the T6SS2s in different *V. parahaemolyticus* isolates are active under similar conditions, clinical strain RIMD2210633-derived POR1, one environmental non-AHPND strain, and four toxic AHPND strains were selected, and the expression and secretion of the T6SS2 hallmark secreted protein Hcp2 were monitored. Similar to POR1, non-AHPND strain A2 and AHPND strains A3, 12297B, and D4 expressed Hcp2 when grown at 23°C, and the expression level of Hcp2 was largely decreased at 37°C (Fig. 2B) (36). AHPND strain 1335 had no detectable level of Hcp2 expression, suggesting that the T6SS2-activating conditions could be different for this isolate (Fig. 2B). Only POR1 and D4 secreted Hcp2 (Fig. 2B). As all strains grew at similar rates at 23°C (see Fig. S2A in the supplemental material), a possible explanation for this result is that additional components necessary for T6SS2 activity are not expressed in these strains under the conditions tested (Fig. 2B). The mechanisms underlying these differences remain unknown and need further characterization.

T6SS1. T6SS1 has previously been associated predominantly with clinical isolates of *V. parahaemolyticus* and shown to possess antibacterial activities against various bac-

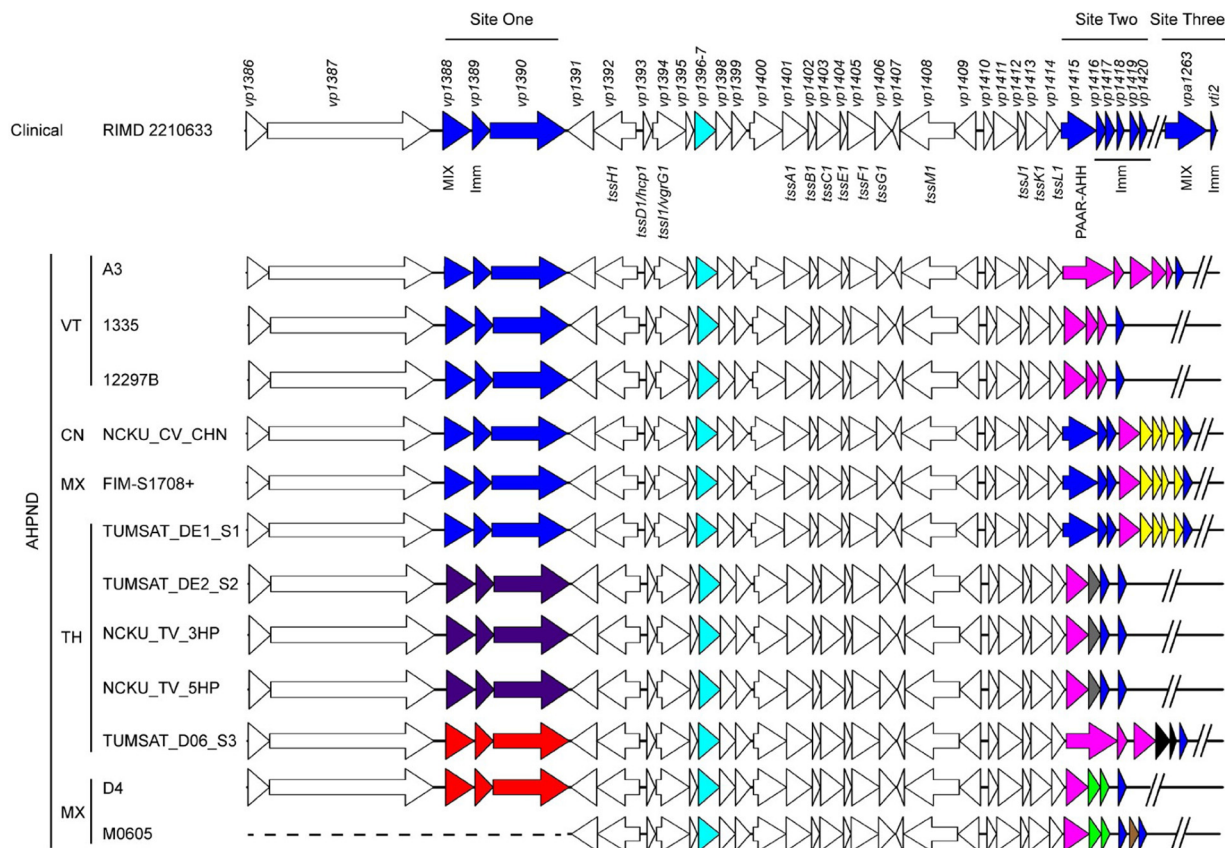


FIG 3 All *V. parahaemolyticus* AHPND strains contain a T6SS1 cluster similar to that of the RIMD2210633 clinical strain. Schematic representation comparison of T6SS1 clusters from clinical and AHPND strains of *V. parahaemolyticus*. RIMD2210633 strain locus numbers are shown above and gene names below. Genes with variations between the strains analyzed are highlighted with different colors. RIMD2210633 genes are labeled in blue, and corresponding genes in AHPND strains are labeled in blue when they are the same or highly conserved but in other colors when otherwise. The same color indicates conserved genes (>90% amino acid identity). In RIMD2210633, the previously annotated *vp1396* and *vp1397* actually form one single gene, as in all AHPND strains (cyan). JP, Japan; VT, Vietnam; TH, Thailand; MX, Mexico; CN, China; MIX, T6SS MIX effector; Imm, immunity protein; AHH, AHH nuclease toxin domain.

terial competitors (36–38). RIMD2210633 T6SS1 is encoded by a main gene cluster (*vp1386-vp1420*) and an orphan E/I module (*vpa1263* and *vti2*) (35, 36). The antibacterial activity of the RIMD2210633 T6SS1 is mediated by at least three effectors: VP1388, VP1415, and VPA1263 (35). VP1388 is a MIX effector encoded at the beginning of the T6SS1 cluster with unknown mechanism of action; VP1415 is a Pro-Ala-Ala-Arg (PAAR) repeat-containing protein with a C-terminal Ala-His-His (AHH) nuclease domain and is encoded at the end of the cluster; VPA1263 is another MIX effector located outside the T6SS1 cluster, which contains pyocin S and colicin DNase domains (Fig. 3) (35). Genes encoding immunity proteins that protect against self-intoxication are encoded downstream of their cognate antibacterial effectors (35). In contrast to previous reports suggesting that T6SS1 is predominantly associated with clinical isolates of *V. parahaemolyticus*, our analysis revealed that all of the 12 toxic AHPND strains analyzed in this study encode a T6SS1 (Fig. 3).

Comparative analysis of the T6SS1s of *V. parahaemolyticus* RIMD2210633 and AHPND strains revealed important variations at three different sites, which are highlighted in blue in the RIMD2210633 T6SS1 cluster shown in Fig. 3. Corresponding genes in the AHPND strains are labeled with blue when they are identical or have greater than 90% identity to the RIMD2210633 proteins and with a different color otherwise. All three sites contain genes encoding the RIMD2210633 T6SS1 effectors, consistent with previous observations showing that the T6SS1 effector repertoire varies between different *V. parahaemolyticus* isolates (41, 42).

Site one encompasses genes *vp1388-vp1390*. VP1388 is a MIX effector, and VP1389 is its cognate immunity protein (35). VP1390 is a protein with unknown function that is secreted in a T6SS1-dependent manner and contains a predicted peptidoglycan-binding domain similar to the C-terminal domain of outer membrane protein OmpA (35). Six of 12 AHPND strains contain the same three genes as those found in RIMD2210633 (Fig. 3). TUMSAT_DE2_S2, NCKU_TV_3HP, and NCKU_TV_5HP contain a different set of three homologous genes, labeled in purple, whereas strains TUMSAT_D06_S3 and D4 possess another set of homologous genes, labeled in red (Fig. 3). In all three sets of genes found as an operon in site one, there are three genes that encode a MIX effector, followed by a putative immunity protein and a large hypothetical protein with unknown function containing a predicted peptidoglycan-binding domain similar to the C-terminal domain of OmpA. A similar observation was recently made in a genomic analysis of virulent *V. parahaemolyticus* strains encoding T6SS1 (41). The beginning of the T6SS1 cluster that contains site one is missing in the genome sequencing data of strain M0605, which was therefore not included in this analysis (Fig. 3).

Site two encompasses *vp1415-vp1420*. VP1415 is a T6SS1 effector, and VP1416 was shown to mediate immunity against it (35). Interestingly, VP1417-VP1420 appear to be distant homologues of the VP1416 immunity protein and could therefore be the result of gene duplications that evolved to provide immunity against homologous AHH nuclease toxins, similar to VP1415. Site two is highly diverse among the AHPND strains, encoding either a single effector protein containing the PAAR and AHH nuclease domains, similar to VP1415 (PAAR-AHH), or two separate proteins (PAAR and AHH). In the latter case, the first protein is the same in all strains and contains the PAAR domain while the second protein varies but retains a nuclease domain (Fig. 3). In addition, site two may include more than one nuclease-containing gene, suggesting multiple T6SS1 E/I pairs (see Fig. S1, versions 1, 3, and 5, in the supplemental material). Furthermore, site two also varies in the number of VP1416-homologous immunity proteins that it encodes (Fig. 3 and Fig. S1). Overall, seven different versions of site two were found in the 12 AHPND strains we examined (Fig. S1).

Site three contains the E/I pair *vpa1263* and *vti2* (35). In RIMD2210633, this module is found outside the T6SS1 cluster within the *V. parahaemolyticus* island 6 (*vpa1254-vpa1270*), a mobile element flanked by a transposase and an integrase located on chromosome 2 (42, 43). Notably, a predicted toxin/antitoxin module containing a putative HNH nuclease toxin (*vpa1260*) and a HigA-like antitoxin (*vpa1259*) is also encoded within the same mobile element (as predicted by HHpred [44]). However, none of the analyzed AHPND strains contain this mobile element with this MIX effector.

We also found that *vp1396* and *vp1397*, which are annotated as two separate genes within the RIMD2210633 T6SS1 gene cluster, are actually one single gene. In all 12 AHPND strains of *V. parahaemolyticus* that we analyzed, the region between *vp1395* and *vp1398* contains one gene that is predicted to encode a single protein, which appears to be a fusion protein of the predicted VP1396 and VP1397 of RIMD2210633. This observation prompted us to determine the source of this discrepancy. To this end, we amplified and then sequenced the region containing *vp1396* and *vp1397* from RIMD2210633. The sequencing results revealed that the current sequence of RIMD2210633 deposited in the NCBI database (NC_004603) includes a wrongly inserted 22-bp fragment, which resulted in the annotation of two separate genes, *vp1396* and *vp1397*. After correcting this error in the sequence, we confirmed that the region between *vp1395* and *vp1398* in RIMD2210633 contains only a single gene that is predicted to encode the same protein as the corresponding region in all of the AHPND strains (Fig. 3, cyan).

Mobile T6SS1 MIX effectors. T6SS MIX effectors are grouped into five distinct clans (35). Members of the MIX V clan were shown to be “orphan” effectors encoded outside T6SS clusters, usually in regions next to mobile genetic elements, and were thus suggested to be horizontally shared between bacteria (35, 42). One such example is

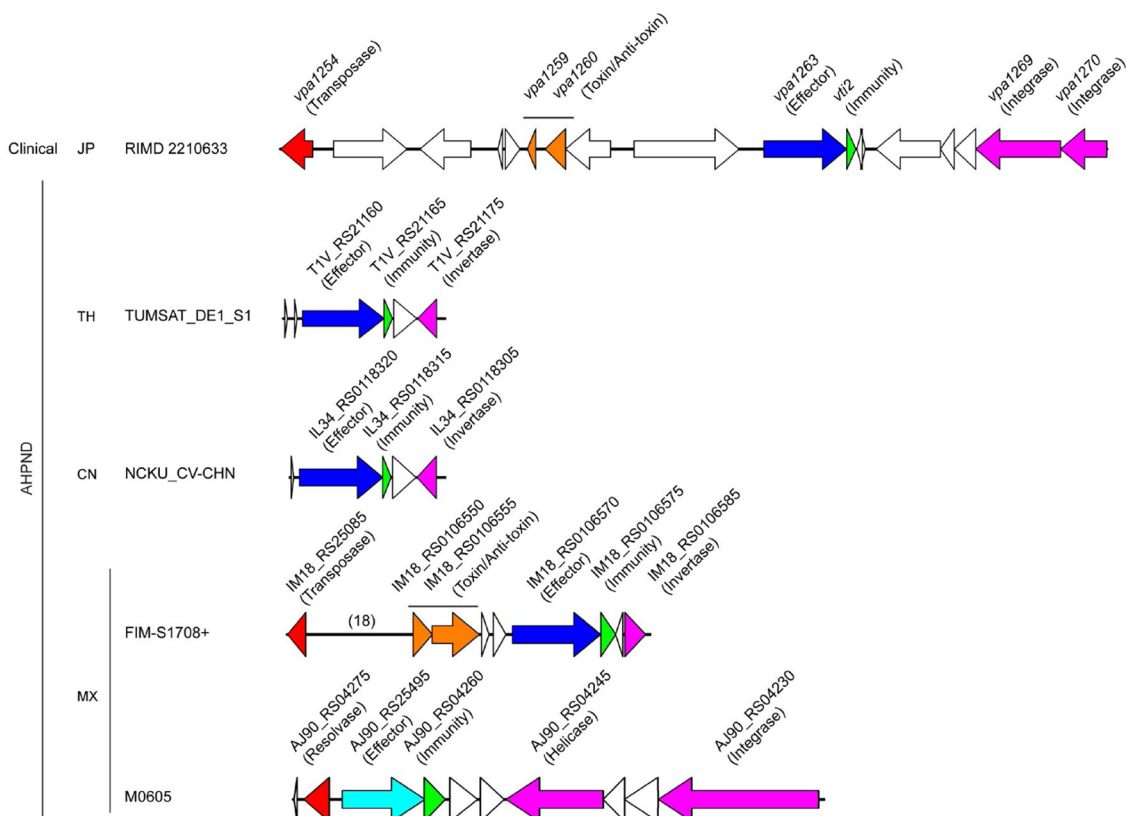


FIG 4 AHPND-causing *V. parahaemolyticus* strains encode mobile T6SS MIX effectors. Mobile genetic elements containing T6SS MIX effectors from the clinical isolate RIMD2210633 and four AHPND strains, including TUMSAT_DE1_S1, NCKU_CV_CHN, FIM-S1708+, and M0605. Components within the mobile elements that are discussed in the text are highlighted with different colors: T6SS mobile MIX effector, blue and cyan; immunity proteins, green; toxin/antitoxin module, orange; genes encoding proteins that mediate DNA rearrangement and mobility upstream of the E/I pair are in red and downstream of the E/I pair are in magenta. The number of omitted genes is shown in parentheses.

vpa1263 in RIMD2210633, which is located on an apparent prophage flanked by a transposase and an integrase (35, 42, 43). Since none of the toxic AHPND strains seem to encode a VPA1263 homologue at the same synteny as in RIMD2210633 (site three), we tested whether any of the AHPND strains contains other mobile T6SS MIX effectors. We searched the protein libraries of all 12 AHPND strains using the MIX domain as our query to identify MIX effectors encoded by genes outside the main T6SS1 gene cluster (35). Our analysis revealed that four AHPND strains, TUMSAT_DE1_S1, NCKU_CV_CHN, FIM-S1708+, and M0605, possess one MIX effector belonging to clan V (Fig. 4). The mobile effectors from TUMSAT_DE1_S1, NCKU_CV_CHN, and FIM-S1708+ all contain the pyocin S and colicin DNase domains, similar to VPA1263 found in RIMD2210633. The effectors in TUMSAT_DE1_S1 and NCKU_CV_CHN are identical and found in the same synteny. M0605 contains a novel mobile MIX effector with a predicted LysM domain and a C-terminal pore-forming toxin domain (as predicted by HHpred [44]). All of the identified MIX effectors had a small open reading frame downstream that is predicted to encode their cognate immunity protein (Fig. 4).

We noticed two features of interest in the genetic neighborhood of these mobile MIX effectors. First, consistent with our previous report on mobile MIX effectors that belong to the MIX V clan, these E/I pairs are flanked by transposable elements (Fig. 4) (42). Genes encoding transposase or resolvase, labeled in red in Fig. 4, are found upstream of the E/I pairs. Downstream of the E/I pairs, there are genes encoding integrase, invertase, or helicase, shown in magenta in Fig. 4. For TUMSAT_DE1_S1 and NCKU_CV_CHN, no genes encoding transposase or resolvase are discovered upstream of the mobile MIX effector. Nevertheless, the assembled contig from their genome

sequences starts with two and one tRNA genes, respectively. Second, we found that the mobile genetic elements containing the mobile MIX effector of both the RIMD2210633 and FIM-51708+ strains also contain genes encoding putative toxin/antitoxin modules upstream of the MIX effector (Fig. 4, orange). We predict that such toxin/antitoxin modules might provide an effective mechanism for bacteria to maintain these mobile genetic elements and thus also maintain the mobile MIX effectors in the genome.

The antibacterial T6SS1 is functional in AHPND-causing *Vibrio parahaemolyticus*. RIMD2210633 T6SS1 is induced under high-salt (3% NaCl) conditions at 30°C when surface sensing is activated (36). Surface sensing can be mimicked when bacteria are grown in suspension by adding phenamil, an inhibitor of the flagellar sodium channel (36). To test whether the T6SS1 in toxic AHPND-causing *V. parahaemolyticus* strains is active and regulated similarly to T6SS1 in the clinical RIMD2210633 isolate, four AHPND isolates were selected and the expression and secretion of the T6SS1 hallmark secreted protein VgrG1 were monitored. A POR1 derivative in which *vgrG1* was deleted was used as a negative control. As shown in Fig. 5A, AHPND-causing strains A3, 1335, 12297B, and D4 all expressed and secreted VgrG1 when grown under T6SS1-inducing conditions, similar to the RIMD2210633 derivative POR1. Notably, strain 1335 expressed and secreted VgrG1 at a lower level than the other strains. Next, we tested the antibacterial activities of the T6SS1 in these four AHPND strains. To do so, we employed bacterial competition assays. AHPND strains A3, D4, and 12297B killed *Escherichia coli* (Fig. 5B) and *Vibrio cholerae* (Fig. 5C) prey similarly to the POR1 positive control. Surprisingly, however, strain 1335 did not show any effect and resembled the POR1/ Δ *hcp1* (T6SS1⁻) negative control (Fig. 5B and C). Notably, the growth rates of POR1 and all four AHPND strains were similar under assay conditions (see Fig. S2B in the supplemental material). Therefore, the mechanism underlying the lack of antibacterial activities in strain 1335 needs further characterization and is likely related to lower levels of T6SS1 activation under the examined conditions, as indicated by lower VgrG1 expression and secretion (Fig. 5A).

To further demonstrate that the bacterial killing was mediated by T6SS1, we performed the competition assay at 37°C, a temperature at which T6SS1 should be inactive (36). As a positive control for bacterial killing at 37°C, we used *Vibrio alginolyticus*, which employs an antibacterial T6SS2 at this temperature (42). Except for D4, none of the *V. parahaemolyticus* strains were able to kill *V. cholerae* at 37°C (see Fig. S3A in the supplemental material), suggesting that T6SS1 activity was required for the observed bactericidal activity at 30°C. Interestingly, even though D4 retained bactericidal activity at 37°C, it is unlikely that this activity was mediated by either T6SS1 or T6SS2, as we did not detect VgrG1 or Hcp2 expression and secretion at this temperature (Fig. S3B and C). Thus, it is possible that D4 possesses additional bactericidal mechanisms not present in the other *V. parahaemolyticus* strains that were examined.

DISCUSSION

AHPND is a newly emerging shrimp disease that has generated devastating losses on the global shrimp industry (1, 2). Identification of the plasmid-encoded binary toxins PirA^{VP}/PirB^{VP} as the deadly cause of AHPND provided significant insights into the mechanism of this disease. However, to enable prevention of AHPND and design effective therapeutic strategies, it is necessary to gain a better understanding of the mechanisms used by these *V. parahaemolyticus* strains to colonize and thrive in the shrimp environment. In this study, we conducted a comparative analysis of the genome sequences for clinical and environmental non-AHPND and toxic AHPND strains of *V. parahaemolyticus* and identified an antibacterial T6SS as a differentiating factor between pathogenic and nonpathogenic strains.

The AHPND strains contain a plasmid with the *pndA* toxin/antitoxin system, ensuring the acquisition of this selfish plasmid in bacterial progeny for survival (8). Genes *pirA*^{VP} and *pirB*^{VP} are flanked by two copies of a gene that encode a transposase, suggesting the possibility that the toxin genes were acquired by the plasmid from some unknown foreign resource (8, 12). The PirA^{VP}/PirB^{VP} toxins from different AHPND strains of *V.*

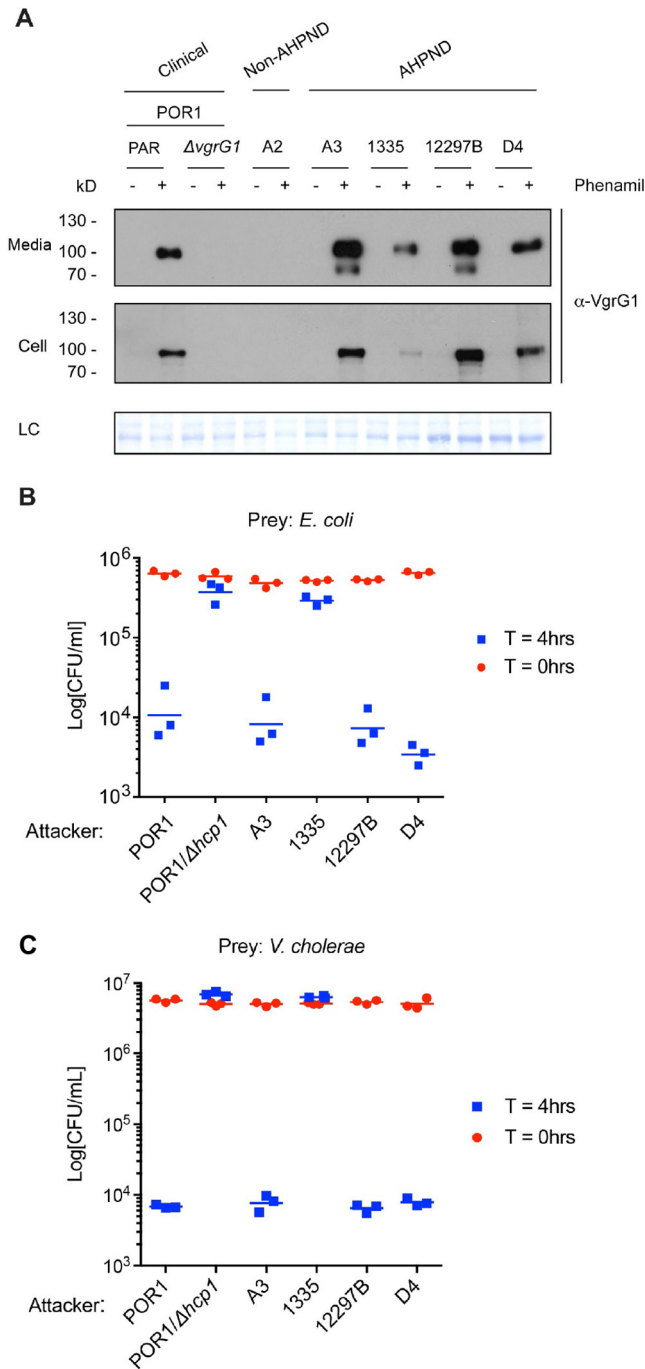


FIG 5 AHPND-causing *V. parahaemolyticus* strains contain a functional antibacterial T6SS1. (A) Expression (Cell) and secretion (Media) of T6SS1 component VgrG1 by the indicated *V. parahaemolyticus* strains grown in MLB at 30°C ± 20 μM phenamil were analyzed by Western blotting using α-VgrG1 antibody. PAR, parental strain. LC, loading control. (B and C) Viability counts of *E. coli* (B) or *V. cholerae* (C) prey before (0 h) and after (4 h) coculture with indicated *V. parahaemolyticus* attacker strains on MLB (3% NaCl) solid media at 30°C. Data are representative of three independent experiments.

parahaemolyticus contain identical protein sequences, indicating that they may have originated from the same source. As noted above, PirA^{VP}/PirB^{VP} are homologues of insecticidal toxins PirA/PirB present in the *Photorhabdus* and *Xenorhabdus* bacterial species (28% sequence identity; see Fig. S4 in the supplemental material). Interestingly, insect-pathogenic bacteria, including *Photorhabdus* and *Xenorhabdus* species, are commonly studied and developed as biological agents for pest control (45). It prompts us

to consider the possibility that the spread of *Photorhabdus* and *Xenorhabdus* in the environment may have facilitated the transfer, directly or via an intermediate, of PirA/PirB toxins into *V. parahaemolyticus*, which leads to the emergence of AHPND. The conjugative transfer and mobilization genes carried on this toxic plasmid could facilitate its spread to *V. parahaemolyticus* strains all over world and to other *Vibrio* species (8, 10, 11).

All of the *V. parahaemolyticus* strains analyzed in this study contain a highly conserved T3SS1 that has been discovered in all sequenced isolates of *V. parahaemolyticus* (Fig. 1A) (24). Similar to clinical isolate RIMD2210633-derived POR1, infection of HeLa cells by non-AHPND strain A2 and the four AHPND strains A3, 1335, 12297B, and D4 showed that their T3SS1 was active and exhibited cytotoxicity (Fig. 1B). It is speculated that maintenance of the T3SS1 contributes to survival of *V. parahaemolyticus* in the environment; however, its natural target remains unknown (25). Notably, except for the clinical isolate RIMD2210633, none of the strains used in this study possess T3SS2 or TDH/TRH toxins. As T3SS2, rather than T3SS1, appears to be the main virulence factor responsible for gastroenteritis in mammals (28), it would be reasonable to conclude that the AHPND-causing isolates do not pose a risk for humans.

A highly conserved T6SS2 was found in all of the *V. parahaemolyticus* strains analyzed in this study (Fig. 2A). However, it appears that the environmental conditions and cues required to activate this system differ between the previously characterized clinical strain RIMD221063 and the non-AHPND- and AHPND-causing strains. Consistent with this observation, it has been recently shown that the regulation of the *V. cholerae* T6SS differs between clinical and environmental isolates, thus suggesting a different requirement for this system in various bacterial lifestyles (46). This may also be the case for T6SS2 in *V. parahaemolyticus*. To understand the mechanisms underlying these differences, further characterization of the conditions and cues that activate the *V. parahaemolyticus* T6SS2 in different strains, as well as its role, will be required.

T6SS1 was previously regarded as being predominantly associated with clinical isolates of *V. parahaemolyticus* (36–38). However, here we show that the antibacterial T6SS1 is present in all 12 AHPND-causing *V. parahaemolyticus* strains used in our study, whereas none of the non-AHPND strains contains T6SS1. Moreover, T6SS gene clusters homologous to the *V. parahaemolyticus* T6SS1 are also found in the genomes of the non-*V. parahaemolyticus* vibrios that cause AHPND (AKQ11_RS16920-17050 in *V. campbellii* KC13.17.5 and TY62_RS02625-02490 in *Vibrio owensii* SH-14). Therefore, we propose that the T6SS1 may not simply be enriched in clinical isolates but is actually linked to *V. parahaemolyticus* virulence, regardless of the target host (humans in clinical isolates and shrimp in AHPND-causing isolates). Given this distinguishing feature, it is likely that T6SS1 plays an important role during infection by killing competitor bacteria and thereby provides a growth advantage for AHPND-causing *V. parahaemolyticus* strains during host colonization. In support of this hypothesis, transcription of the *V. parahaemolyticus* T6SS1 was previously shown to be induced during animal infection, suggesting that this antibacterial T6SS1 provides an advantage inside the host (47). Indeed, we demonstrate that three AHPND-causing strains (A3, 12297B, and D4) possess a functional antibacterial T6SS1. Surprisingly, another AHPND-causing strain, 1335, was unable to kill *E. coli* and *V. cholerae* prey in a bacterial competition assay, even though it encodes a T6SS1 with at least two antibacterial effectors. This inability to mediate antibacterial activities could be explained by a lower activity level of T6SS1 than in the other tested strains, as we observed while monitoring the expression and secretion of the hallmark secreted protein VgrG1 (Fig. 5A). It is therefore possible that the environmental conditions required to fully activate T6SS1 in strain 1335 are slightly different from the ones sufficient to activate the system in other strains but that the ideal conditions do exist in the shrimp host. Alternatively, it is possible that this strain acquired other determinants that aid it in establishing a niche inside the host, thus making the T6SS1-mediated antibacterial activities nonessential.

We and others previously reported that T6SS effector repertoires may vary among different isolates of the same bacterial species (42, 48). Whereas a previous study found

high variances only in the site encoding the VP1388 MIX effector between different *V. parahaemolyticus* strains (named “site one” in this work) (41), our comparison of the T6SS1s from RIMD2210633 and all of the AHPND strains revealed three highly divergent sites, all of which correspond to the locations of the three known *V. parahaemolyticus* RIMD2210633 antibacterial effectors (35). This type of rapid evolution of T6SS E/I pairs in different *V. parahaemolyticus* isolates provides a molecular explanation to our previous observation showing that the *V. parahaemolyticus* T6SS1 mediates not only interspecies competition but also intraspecies competition (36). Moreover, we previously demonstrated that marine bacteria, and especially vibrios, share T6SS effectors that belong to the MIX V clan of MIX effectors via horizontal gene transfer (42). Indeed, when we searched the genomes of the AHPND-causing strains for MIX effectors, we discovered that each of the four AHPND strains, TUMSAT_DE1_S1, NCKU_CV_CHN, FIM-S1708+, and M0605, contains one “orphan” (i.e., not carried within the main T6SS gene cluster) MIX-E/I pair. In agreement with our previous report, these four novel *V. parahaemolyticus* MIX effectors are located within mobile genetic elements that contain genes encoding proteins involved in DNA rearrangement and mobility (42). Furthermore, they all belong to the mobile MIX V clan. Interestingly, the MIX effector-containing mobile genetic elements of both RIMD2210633 and FIM-S1708+ also possess genes that encode a toxin/antitoxin module, providing a possible effective mechanism for the maintenance of these mobile units. As we have shown previously, acquisition of these novel mobile MIX effectors provides a competitive advantage over neighboring kin bacteria (42). A bacterium that acquires a novel antibacterial MIX effector on a mobile genetic element is able to outcompete its kin and establish itself in the population. Thus, such mobile MIX effectors can be a driving force for the evolution of these pathogen populations (42, 49, 50). Moreover, we propose that the rapidly evolving T6SS1 E/I pairs that we found in this work may play a significant role in the worldwide dissemination of AHPND-causing *V. parahaemolyticus* strains, as they can enhance their environmental competitive fitness (1, 42).

In conclusion, our studies revealed different repertoires of putative virulence factors that distinguish non-AHPND from AHPND-causing *V. parahaemolyticus* strains. In addition to the acquisition of the plasmid-borne binary toxins PirA^{VP}/PirB^{VP}, which mediate virulence against shrimp, the virulent *V. parahaemolyticus* strains seem to have acquired a selective competitive advantage over other bacterial strains, the T6SS1, that enhances their environmental fitness. This antibacterial T6SS1 may play a major role in the emerging shrimp disease AHPND, as it could be required for *V. parahaemolyticus* to establish a replicative niche inside the host.

MATERIALS AND METHODS

Bacterial strains and media. *V. parahaemolyticus* non-AHPND strain A2 and AHPND strains A3, 1335, 12297B, and D4 are generous gifts from Donald Lightner at the University of Arizona and were used for bacterial whole-genome sequencing and in the experiments described here. The *V. parahaemolyticus* strains used in this study, from five geographical origins, i.e., Japan (JP), Vietnam (VT), Thailand (TH), Mexico (MX), and China (CN), are as follows: (i) a clinical strain from Japan, strain RIMD2210633; (ii) five non-AHPND strains, including 1 from Vietnam (strain A2), 3 from Thailand (strains TUMSAT_H01_S4, TUMSAT_H10_S6, and NCKU_TN_S02), and 1 from Mexico (strain FIM-S1392-); (iii) 12 AHPND-causing strains, including 3 from Vietnam (strains A3, 1335, and 12297B), 5 from Thailand (strains TUMSAT_DE1_S1, TUMSAT_DE2_S2, TUMSAT_D06_S3, NCKU_TV_3HP, and NCKU_TV_5HP), 1 from China (strain NCKU_CV_CHN), and 3 from Mexico (strains D4, M0605, and FIM-S1708+). POR1 (RIMD2210633 Δ tdhA5) is a derivative strain of the clinical isolate RIMD2210633 (29, 51). POR2 (POR1 Δ vcrD1) and POR3 (POR1 Δ vcrD2) were used as controls lacking a functional T3SS1 and T3SS2, respectively (29). *V. alginolyticus* strain 12G01 was used in bacterial competition assays (see below). All *V. parahaemolyticus* and *V. alginolyticus* strains were routinely cultured in marine Luria-Bertani (MLB) broth (Luria-Bertani broth containing 3% NaCl) or on marine minimal medium (MMM) agar (1.5% [wt/vol] agar, 2% [wt/vol] NaCl, 0.4% [wt/vol] galactose, 5 mM MgSO₄, 7 mM K₂SO₄, 77 mM K₂HPO₄, 35 mM KH₂PO₄, 2 mM NH₄Cl) at 30°C. *V. cholerae* strain El Tor N16961 was used as prey in bacterial competition assays (see below) and was grown in LB at 37°C. *E. coli* strain DH5 α was used as prey for bacterial competition assays (see below). *E. coli* strain S17-1 (λ pir) was used for maintenance of pDM4 plasmids and mating (see below). *E. coli* strains were routinely cultured in 2 \times YT broth (1.6% [wt/vol] tryptone, 1% [wt/vol] yeast extract, 0.5% [wt/vol] NaCl) at 37°C with addition of chloramphenicol (25 μ g/ml) when maintenance of plasmid was required.

Construction of deletion strains. For in-frame deletions of *vgrG1* (locus tag *vp1394*) and *hcp2* (locus tag *vpa1027*), 1-kb sequences directly upstream and downstream of each gene were cloned into pDM4, a *Cm^r* OriR6K suicide plasmid (52). These pDM4 constructs were inserted into *V. parahaemolyticus* via conjugation by *E. coli* S17-1 (λ *pir*). Transconjugants were selected for on MMM agar containing chloramphenicol. The resulting transconjugants were plated onto MMM agar containing 15% (wt/vol) sucrose for counterselection and loss of the *sacB*-containing pDM4. Deletions were confirmed by PCR. The generation of in-frame deletions of *hcp1* (locus tag *vp1393*) was described previously (36).

Antibodies. Polyclonal antibodies were produced in-house with rabbits for the VgrG1 (VP1394) peptide KDMSTKVLNRRYRDIGQDE and the Hcp2 (VPA1027) peptide KYADIKGEATAEQ.

Next-generation sequencing (NGS) and bacterial genome assembly and annotation. Whole-genome sequencing of *V. parahaemolyticus* was conducted using the homopolymer tail-mediated ligation PCR (HTML-PCR) method followed by single-end 50-nucleotide sequencing performed on the Illumina HiSeq2500 (53).

For bacterial genome assembly, the sequencing reads for each sample were processed sequentially by mirabait (version 3.4.0) (54) to remove contamination from the Illumina sequencing adapters, by fastq_quality_trimmer from the FASTX toolkit (version 0.0.13; http://hannonlab.cshl.edu/fastx_toolkit/) to remove low-quality base pairs at both ends, and by Jellyfish (version 1.1.2) (55) to obtain 15-mer frequencies in the reads. The 15-mers with frequencies much lower than expected probably contained sequencing errors and were corrected using Quake (56). The error-corrected reads were assembled into contigs using SOAPdenovo2 (version 2.044r240) (57). The assembled whole-genome sequence was then annotated by RAST (Rapid Annotation using Subsystem Technology) to generate the protein library (58).

Identification of mobile T6SS MIX effectors. We generated a BLAST database library using genome-wide protein sequences from all *V. parahaemolyticus* strains examined in this study using the makeblastdb application. To identify potential T6SS MIX effectors, we searched the strain library using all available MIX effector protein sequences from previous studies as queries (BLAST E value cutoff, 0.001) (35, 59). We removed redundant hits and identified MIX V-like protein sequences in four AHPND strains, FIM-S1708+, M0605, NCKU_CV_CHN, and TUMSAT_DE1_S1.

LDH cytotoxicity assay. HeLa cells were plated in a 24-well tissue culture plate at 8×10^4 cells per well and grown for 24 h. *V. parahaemolyticus* strains POR1, A2, A3, 1335, 12297B, and D4 were grown in MLB medium at 30°C overnight. Overnight bacterial cultures were diluted with DMEM to an optical density at 600 nm (OD_{600}) of 0.3 and grown at 37°C for 30 min to induce T3SS1. Induced *V. parahaemolyticus* isolates were then used to infect HeLa cells at a multiplicity of infection (MOI) of 10. At 4 h postinfection, lactate dehydrogenase (LDH) release into the culture medium was evaluated as a measure of cytotoxicity and host cell lysis by using a colorimetric cytotoxicity detection kit (TaKaRa Bio) according to the manufacturer's instructions. Assays were repeated at least three times with similar results, and results of a representative experiment are shown.

T6SS2 expression and secretion assay. *V. parahaemolyticus* strains were grown in MLB at 30°C overnight. To test the activity of T6SS2 under low-salt conditions, overnight bacterial cultures were diluted to an OD_{600} of 0.9 in LB and grown at 23°C or 37°C for 5 h, as previously described (36). For the expression fraction (cell), bacterial cultures with the same OD_{600} were collected and cell pellets were resuspended in 2 \times protein sample buffer (100 mM Tris-HCl [pH 6.8], 20% glycerol, 2% sodium dodecyl sulfate [SDS], 2% β -mercaptoethanol, 150 mM sodium hydroxide, bromophenol blue). For the secretion fraction (Media), bacterial culture supernatants were filtered with a 0.22- μ m filter and precipitated with deoxycholate and trichloroacetic acid (60). Precipitated proteins were pelleted, washed twice with acetone, and then resuspended in 2 \times protein sample buffer. Hcp2 expression and secretion were detected by Western blot analysis. Total protein load was assessed by staining the membrane of the cell fractions with Coomassie blue (Fig. 2) or Ponceau S (Fig. S3). Assays were performed at least three times with similar results, and the results of a representative experiment are shown.

T6SS1 expression and secretion assay. *V. parahaemolyticus* strains were grown in MLB at 30°C overnight. Overnight bacterial cultures were diluted to an OD_{600} of 0.18 in MLB and grown at 30°C for 5 h. Phenamil (20 μ M) was added when necessary to induce T6SS1 (36). Pellet and supernatant samples were treated as described above for T6SS2 expression and secretion assay. VgrG1 expression and secretion were detected by Western blot analysis. Total protein load was assessed by staining the membrane of the cell fractions with Coomassie blue (Fig. 5) or Ponceau S (Fig. S3). Assays were performed at least three times with similar results, and the results of a representative experiment are shown.

Bacterial competition assay. Bacterial strains were grown overnight in MLB (for *V. parahaemolyticus* and *V. alginolyticus*), 2 \times YT (for *E. coli* DH5 α), or LB (for *V. cholerae*). Bacterial cultures were mixed in triplicates at a 4:1 (attacker-to-prey) ratio and spotted onto MLB (3% NaCl) plates as previously described (36). CFU of the prey spotted at time zero ($t = 0$ h) were determined by plating 10-fold serial dilutions onto selective LB medium plates (containing 25 μ g/ml chloramphenicol for selection of *E. coli* prey containing a pBAD33 plasmid for antibiotic resistance or 50 μ g/ml streptomycin for selection of *V. cholerae* prey). Bacterial spots were harvested after 4 h of incubation at either 30°C or 37°C, and the CFU of the surviving prey cells were determined as explained above. Assays were repeated three times with similar results, and results of a representative experiment are shown.

Bacterial growth assay. Triplicates of overnight cultures of *V. parahaemolyticus* strains were normalized to an OD_{600} of 0.1 in MLB (3% NaCl) and grown at 30°C or in LB (1% NaCl) and grown at 23°C. Growth was measured as OD_{600} . The assay was repeated three times with similar results, and results of a representative experiment are shown.

Identification of virulence factors (PirA/B, TDH/TRH, T3SS, and T6SS) in *V. parahaemolyticus* non-AHPND and AHPND strains. *V. parahaemolyticus* genes encoding PirA/B, TDH/TRH, and conserved components of T3SS and T6SS were used as the templates to search against assembled genomes of non-AHPND and AHPND strains analyzed in this study for corresponding genes encoding these virulence factors. The entire T3SS and T6SS clusters in the non-AHPND and AHPND strains were identified by analyzing adjacent genes flanking the conserved components mentioned above. Then, the similarity between RIMD221063 genes and those in the other *V. parahaemolyticus* strains was assessed using BLAST. In general, genes with over 90% identities based on BLAST analysis were considered conservative and labeled with the same color; otherwise, they were labeled with different colors.

Accession number(s). The accession numbers of the sequences determined in this study have been deposited in GenBank as follows: strain A2, [MWVH00000000](https://doi.org/10.1093/genbank/MWVH00000000); strain 1335, [MYFF00000000](https://doi.org/10.1093/genbank/MYFF00000000); strain 12297B, [MYFG00000000](https://doi.org/10.1093/genbank/MYFG00000000); strain D4, [MYFH00000000](https://doi.org/10.1093/genbank/MYFH00000000).

SUPPLEMENTAL MATERIAL

Supplemental material for this article may be found at <https://doi.org/10.1128/AEM.00737-17>.

SUPPLEMENTAL FILE 1, PDF file, 1.4 MB.

ACKNOWLEDGMENTS

We thank members of the Orth lab for their expert advice and editing.

This work was funded in part by the National Institutes of Health (NIH) grant GM094575 and the Welch Foundation grant I-1505 (N.V.G.); by NIH grant R01-AI056404, the Welch Foundation grant I-1561, and Once Upon a Time. (K.O.); and by NIH grant R01-AI055058 (A.C.). K.O. is a Burroughs Wellcome Investigator in Pathogenesis of Infectious Disease, a Beckman Young Investigator, and a W. W. Caruth, Jr., Biomedical Scholar and has an Earl A. Forsythe Chair in Biomedical Science. D.S. is an Alon Fellow. The funders had no role in study design, data collection and analysis, decision to publish, or preparation of the manuscript.

REFERENCES

- Tran L, Nunan L, Redman RM, Mohney LL, Pantoja CR, Fitzsimmons K, Lightner DV. 2013. Determination of the infectious nature of the agent of acute hepatopancreatic necrosis syndrome affecting penaeid shrimp. *Dis Aquat Organ* 105:45–55. <https://doi.org/10.3354/dao02621>.
- Lai HC, Ng TH, Ando M, Lee CT, Chen IT, Chuang JC, Mavichak R, Chang SH, Yeh MD, Chiang YA, Takeyama H, Hamaguchi HO, Lo CF, Aoki T, Wang HC. 2015. Pathogenesis of acute hepatopancreatic necrosis disease (AHPND) in shrimp. *Fish Shellfish Immunol* 47:1006–1014. <https://doi.org/10.1016/j.fsi.2015.11.008>.
- de la Pena LD, Cabillon NA, Catedral DD, Amar EC, Usero RC, Monotilla WD, Calpe AT, Fernandez DD, Saloma CP. 2015. Acute hepatopancreatic necrosis disease (AHPND) outbreaks in *Penaeus vannamei* and *P. monodon* cultured in the Philippines. *Dis Aquat Organ* 116:251–254. <https://doi.org/10.3354/dao02919>.
- Gomez-Gil B, Soto-Rodriguez S, Lozano R, Betancourt-Lozano M. 2014. Draft genome sequence of *Vibrio parahaemolyticus* strain M0605, which causes severe mortalities of shrimps in Mexico. *Genome Announc* 2(2): e00055-14. <https://doi.org/10.1128/genomeA.00055-14>.
- Nunan L, Lightner D, Pantoja C, Gomez-Jimenez S. 2014. Detection of acute hepatopancreatic necrosis disease (AHPND) in Mexico. *Dis Aquat Organ* 111:81–86. <https://doi.org/10.3354/dao02776>.
- Restrepo L, Bayot B, Betancourt I, Pinzon A. 2016. Draft genome sequence of pathogenic bacteria *Vibrio parahaemolyticus* strain Ba94C2, associated with acute hepatopancreatic necrosis disease isolate from South America. *Genom Data* 9:143–144. <https://doi.org/10.1016/j.gdata.2016.08.008>.
- De Schryver P, Defoirdt T, Sorgeloos P. 2014. Early mortality syndrome outbreaks: a microbial management issue in shrimp farming? *PLoS Pathog* 10(4):e1003919. <https://doi.org/10.1371/journal.ppat.1003919>.
- Lee CT, Chen IT, Yang YT, Ko TP, Huang YT, Huang JY, Huang MF, Lin SJ, Chen CY, Lin SS, Lightner DV, Wang HC, Wang AH, Wang HC, Hor LI, Lo CF. 2015. The opportunistic marine pathogen *Vibrio parahaemolyticus* becomes virulent by acquiring a plasmid that expresses a deadly toxin. *Proc Natl Acad Sci U S A* 112:10798–10803. <https://doi.org/10.1073/pnas.1503129112>.
- Sirikharin R, Taengchaiyaphum S, Sanguanrut P, Chi TD, Mavichak R, Proespraiwong P, Nuangsaeng B, Thitamadee S, Flegel TW, Sritunyaluck-sana K. 2015. Characterization and PCR detection of binary, Pir-like toxins from *Vibrio parahaemolyticus* isolates that cause acute hepatopancreatic necrosis disease (AHPND) in shrimp. *PLoS One* 10(5):e0126987. <https://doi.org/10.1371/journal.pone.0126987>.
- Kondo H, Van PT, Dang LT, Hirono I. 2015. Draft genome sequence of non-*Vibrio parahaemolyticus* acute hepatopancreatic necrosis disease strain KC13.17.5, isolated from diseased shrimp in Vietnam. *Genome Announc* 3(5):e00978-15. <https://doi.org/10.1128/genomeA.00978-15>.
- Liu L, Xiao J, Xia X, Pan Y, Yan S, Wang Y. 2015. Draft genome sequence of *Vibrio owensii* strain SH-14, which causes shrimp acute hepatopancreatic necrosis disease. *Genome Announc* 3(6):e01395-15. <https://doi.org/10.1128/genomeA.01395-15>.
- Xiao J, Liu L, Ke Y, Li X, Liu Y, Pan Y, Yan S, Wang Y. 2017. Shrimp AHPND-causing plasmids encoding the PirAB toxins as mediated by pirAB-Tn903 are prevalent in various *Vibrio* species. *Sci Rep* 7:42177. <https://doi.org/10.1038/srep42177>.
- Broberg CA, Calder TJ, Orth K. 2011. *Vibrio parahaemolyticus* cell biology and pathogenicity determinants. *Microbes Infect* 13:992–1001. <https://doi.org/10.1016/j.micinf.2011.06.013>.
- Zhang L, Orth K. 2013. Virulence determinants for *Vibrio parahaemolyticus* infection. *Curr Opin Microbiol* 16:70–77. <https://doi.org/10.1016/j.mib.2013.02.002>.
- Nair GB, Ramamurthy T, Bhattacharya SK, Dutta B, Takeda Y, Sack DA. 2007. Global dissemination of *Vibrio parahaemolyticus* serotype O3:K6 and its serovariants. *Clin Microbiol Rev* 20:39–48. <https://doi.org/10.1128/CMR.00025-06>.
- Velazquez-Roman J, Leon-Sicairos N, de Jesus Hernandez-Diaz L, Canizalez-Roman A. 2014. Pandemic *Vibrio parahaemolyticus* O3:K6 on the American continent. *Front Cell Infect Microbiol* 3:110. <https://doi.org/10.3389/fcimb.2013.00110>.
- McLaughlin JB, DePaola A, Bopp CA, Martinek KA, Napolilli NP, Allison CG, Murray SL, Thompson EC, Bird MM, Middaugh JP. 2005. Outbreak of *Vibrio parahaemolyticus* gastroenteritis associated with Alaskan oysters. *N Engl J Med* 353:1463–1470. <https://doi.org/10.1056/NEJMoA051594>.

18. O'Boyle N, Boyd A. 2014. Manipulation of intestinal epithelial cell function by the cell contact-dependent type III secretion systems of *Vibrio parahaemolyticus*. *Front Cell Infect Microbiol* 3:114. <https://doi.org/10.3389/fcimb.2013.00114>.
19. Daniels NA, MacKinnon L, Bishop R, Altekruze S, Ray B, Hammond RM, Thompson S, Wilson S, Bean NH, Griffin PM, Slutsker L. 2000. *Vibrio parahaemolyticus* infections in the United States, 1973–1998. *J Infect Dis* 181:1661–1666. <https://doi.org/10.1086/315459>.
20. Vezzulli L, Grande C, Reid PC, Helaouet P, Edwards M, Hofle MG, Brettar I, Colwell RR, Pruzzo C. 2016. Climate influence on *Vibrio* and associated human diseases during the past half-century in the coastal North Atlantic. *Proc Natl Acad Sci U S A* 113:E5062–E5071. <https://doi.org/10.1073/pnas.1609157113>.
21. de Souza Santos M, Salomon D, Li P, Krachler A-M, Orth K. 2015. *Vibrio parahaemolyticus* virulence determinants, p 230–60. In Alouf J, Ladant D, Popoff MR (ed), *The comprehensive sourcebook of bacterial protein toxins*. Elsevier, Waltham, MA.
22. Galan JE, Lara-Tejero M, Marlovits TC, Wagner S. 2014. Bacterial type III secretion systems: specialized nanomachines for protein delivery into target cells. *Annu Rev Microbiol* 68:415–438. <https://doi.org/10.1146/annurev-micro-092412-155725>.
23. Okada N, Iida T, Park KS, Goto N, Yasunaga T, Hiyoshi H, Matsuda S, Kodama T, Honda T. 2009. Identification and characterization of a novel type III secretion system in trh-positive *Vibrio parahaemolyticus* strain TH3996 reveal genetic lineage and diversity of pathogenic machinery beyond the species level. *Infect Immun* 77:904–913. <https://doi.org/10.1128/IAI.01184-08>.
24. Okada N, Matsuda S, Matsuyama J, Park KS, de los Reyes C, Kogure K, Honda T, Iida T. 2010. Presence of genes for type III secretion system 2 in *Vibrio mimicus* strains. *BMC Microbiol* 10:302. <https://doi.org/10.1186/1471-2180-10-302>.
25. Ono T, Park KS, Ueta M, Iida T, Honda T. 2006. Identification of proteins secreted via *Vibrio parahaemolyticus* type III secretion system 1. *Infect Immun* 74:1032–1042. <https://doi.org/10.1128/IAI.74.2.1032-1042.2006>.
26. Burdette DL, Yarbrough ML, Orvedahl A, Gilpin CJ, Orth K. 2008. *Vibrio parahaemolyticus* orchestrates a multifaceted host cell infection by induction of autophagy, cell rounding, and then cell lysis. *Proc Natl Acad Sci U S A* 105:12497–12502. <https://doi.org/10.1073/pnas.0802773105>.
27. Gotoh K, Kodama T, Hiyoshi H, Izutsu K, Park KS, Dryselius R, Akeda Y, Honda T, Iida T. 2010. Bile acid-induced virulence gene expression of *Vibrio parahaemolyticus* reveals a novel therapeutic potential for bile acid sequestrants. *PLoS One* 5(10):e13365. <https://doi.org/10.1371/journal.pone.0013365>.
28. Ritchie JM, Rui H, Zhou X, Iida T, Kodama T, Ito S, Davis BM, Bronson RT, Waldor MK. 2012. Inflammation and disintegration of intestinal villi in an experimental model for *Vibrio parahaemolyticus*-induced diarrhea. *PLoS Pathog* 8(3):e1002593. <https://doi.org/10.1371/journal.ppat.1002593>.
29. Park KS, Ono T, Rokuda M, Jang MH, Okada K, Iida T, Honda T. 2004. Functional characterization of two type III secretion systems of *Vibrio parahaemolyticus*. *Infect Immun* 72:6659–6665. <https://doi.org/10.1128/IAI.72.11.6659-6665.2004>.
30. Hiyoshi H, Kodama T, Iida T, Honda T. 2010. Contribution of *Vibrio parahaemolyticus* virulence factors to cytotoxicity, enterotoxigenicity, and lethality in mice. *Infect Immun* 78:1772–1780. <https://doi.org/10.1128/IAI.01051-09>.
31. Ho BT, Dong TG, Mekalanos JJ. 2014. A view to a kill: the bacterial type VI secretion system. *Cell Host Microbe* 15:9–21. <https://doi.org/10.1016/j.chom.2013.11.008>.
32. Russell AB, Peterson SB, Mougous JD. 2014. Type VI secretion system effectors: poisons with a purpose. *Nat Rev Microbiol* 12:137–148. <https://doi.org/10.1038/nrmicro3185>.
33. Russell AB, Hood RD, Bui NK, LeRoux M, Vollmer W, Mougous JD. 2011. Type VI secretion delivers bacteriolytic effectors to target cells. *Nature* 475:343–347. <https://doi.org/10.1038/nature10244>.
34. Russell AB, Singh P, Brittnacher M, Bui NK, Hood RD, Carl MA, Agnello DM, Schwarz S, Goodlett DR, Vollmer W, Mougous JD. 2012. A widespread bacterial type VI secretion effector superfamily identified using a heuristic approach. *Cell Host Microbe* 11:538–549. <https://doi.org/10.1016/j.chom.2012.04.007>.
35. Salomon D, Kinch LN, Trudgian DC, Guo X, Klimko JA, Grishin NV, Mirzaei H, Orth K. 2014. Marker for type VI secretion system effectors. *Proc Natl Acad Sci U S A* 111:9271–9276. <https://doi.org/10.1073/pnas.1406110111>.
36. Salomon D, Gonzalez H, Updegraff BL, Orth K. 2013. *Vibrio parahaemolyticus* type VI secretion system 1 is activated in marine conditions to target bacteria, and is differentially regulated from system 2. *PLoS One* 8(4):e61086. <https://doi.org/10.1371/journal.pone.0061086>.
37. Yu Y, Yang H, Li J, Zhang P, Wu B, Zhu B, Zhang Y, Fang W. 2012. Putative type VI secretion systems of *Vibrio parahaemolyticus* contribute to adhesion to cultured cell monolayers. *Arch Microbiol* 194:827–835. <https://doi.org/10.1007/s00203-012-0816-z>.
38. Boyd EF, Cohen AL, Naughton LM, Ussery DW, Binnewies TT, Stine OC, Parent MA. 2008. Molecular analysis of the emergence of pandemic *Vibrio parahaemolyticus*. *BMC Microbiol* 8:110. <https://doi.org/10.1186/1471-2180-8-110>.
39. Makino S, Tobe T, Asakura H, Watarai M, Ikeda T, Takeshi K, Sasakawa C. 2003. Distribution of the secondary type III secretion system locus found in enterohemorrhagic *Escherichia coli* O157:H7 isolates among Shiga toxin-producing *E. coli* strains. *J Clin Microbiol* 41:2341–2347. <https://doi.org/10.1128/JCM.41.6.2341-2347.2003>.
40. Park KS, Ono T, Rokuda M, Jang MH, Iida T, Honda T. 2004. Cytotoxicity and enterotoxigenicity of the thermostable direct hemolysin-deletion mutants of *Vibrio parahaemolyticus*. *Microbiol Immunol* 48:313–318. <https://doi.org/10.1128/J.1348-0421.2004.tb03512.x>.
41. Ronholm J, Petronella N, Chew Leung C, Pightling AW, Banerjee SK. 2015. Genomic features of environmental and clinical *Vibrio parahaemolyticus* isolates lacking recognized virulence factors are dissimilar. *Appl Environ Microbiol* 82:1102–1113. <https://doi.org/10.1128/AEM.03465-15>.
42. Salomon D, Klimko JA, Trudgian DC, Kinch LN, Grishin NV, Mirzaei H, Orth K. 2015. Type VI secretion system toxins horizontally shared between marine bacteria. *PLoS Pathog* 11(8):e1005128. <https://doi.org/10.1371/journal.ppat.1005128>.
43. Hurley CC, Quirke A, Reen FJ, Boyd EF. 2006. Four genomic islands that mark post-1995 pandemic *Vibrio parahaemolyticus* isolates. *BMC Genomics* 7:104. <https://doi.org/10.1186/1471-2164-7-104>.
44. Hildebrand A, Rimmert M, Biegert A, Soding J. 2009. Fast and accurate automatic structure prediction with HHpred. *Proteins* 77(Suppl 9):S128–S132. <https://doi.org/10.1002/prot.22499>.
45. Rui L. 2015. Insect pathogenic bacteria in integrated pest management. *Insects* 6:352–367. <https://doi.org/10.3390/insects6020352>.
46. Bernardy EE, Turnsek MA, Wilson SK, Tarr CL, Hammer BK. 2016. Diversity of clinical and environmental isolates of *Vibrio cholerae* in natural transformation and contact-dependent bacterial killing indicative of type VI secretion system activity. *Appl Environ Microbiol* 82:2833–2842. <https://doi.org/10.1128/AEM.00351-16>.
47. Livny J, Zhou X, Mandlik A, Hubbard T, Davis BM, Waldor MK. 2014. Comparative RNA-Seq based dissection of the regulatory networks and environmental stimuli underlying *Vibrio parahaemolyticus* gene expression during infection. *Nucleic Acids Res* 42:12212–12223. <https://doi.org/10.1093/nar/gku891>.
48. Unterwiesing D, Miyata ST, Bachmann V, Brooks TM, Mullins T, Kostiuik B, Provenzano D, Pukatzki S. 2014. The *Vibrio cholerae* type VI secretion system employs diverse effector modules for intraspecific competition. *Nat Commun* 5:3549. <https://doi.org/10.1038/ncomms4549>.
49. Borgeaud S, Metzger LC, Scignari T, Blokesch M. 2015. The type VI secretion system of *Vibrio cholerae* fosters horizontal gene transfer. *Science* 347:63–67. <https://doi.org/10.1126/science.1260064>.
50. Salomon D. 2016. MIX and match: mobile T6SS MIX-effectors enhance bacterial fitness. *Mob Genet Elements* 6(1):e1123796. <https://doi.org/10.1080/2159256X.2015.1123796>.
51. Eagon RG. 1962. *Pseudomonas natriegens*, a marine bacterium with a generation time of less than 10 minutes. *J Bacteriol* 83:736–737.
52. O'Toole R, Milton DL, Wolf-Watz H. 1996. Chemotactic motility is required for invasion of the host by the fish pathogen *Vibrio anguillarum*. *Mol Microbiol* 19:625–637. <https://doi.org/10.1046/j.1365-2958.1996.412927.x>.
53. Lazinski DW, Camilli A. 2013. Homopolymer tail-mediated ligation PCR: a streamlined and highly efficient method for DNA cloning and library construction. *Biotechniques* 54:25–34. <https://doi.org/10.2144/000113981>.
54. Chevreaux B, Wetter T, Suhai S. 1999. Genome sequence assembly using trace signals and additional sequence information, p 45–56. *Computer Science and Biology: proceedings of the German Conference on Bioinformatics*.
55. Marçais G, Kingsford C. 2011. A fast, lock-free approach for efficient parallel counting of occurrences of k-mers. *Bioinformatics* 27:764–770. <https://doi.org/10.1093/bioinformatics/btr011>.

56. Kelley DR, Schatz MC, Salzberg SL. 2010. Quake: quality-aware detection and correction of sequencing errors. *Genome Biol* 11(11):R116. <https://doi.org/10.1186/gb-2010-11-11-r116>.
57. Luo R, Liu B, Xie Y, Li Z, Huang W, Yuan J, He G, Chen Y, Pan Q, Liu Y, Tang J, Wu G, Zhang H, Shi Y, Liu Y, Yu C, Wang B, Lu Y, Han C, Cheung DW, Yiu SM, Peng S, Xiaoqian Z, Liu G, Liao X, Li Y, Yang H, Wang J, Lam TW, Wang J. 2012. SOAPdenovo2: an empirically improved memory-efficient short-read de novo assembler. *Gigascience* 1(1):18. <https://doi.org/10.1186/2047-217X-1-18>.
58. Overbeek R, Olson R, Pusch GD, Olsen GJ, Davis JJ, Disz T, Edwards RA, Gerdes S, Parrello B, Shukla M, Vonstein V, Wattam AR, Xia F, Stevens R. 2014. The SEED and the Rapid Annotation of microbial genomes using Subsystems Technology (RAST). *Nucleic Acids Res* 42(Database issue): D206–D214.
59. Altschul SF, Madden TL, Schaffer AA, Zhang J, Zhang Z, Miller W, Lipman DJ. 1997. Gapped BLAST and PSI-BLAST: a new generation of protein database search programs. *Nucleic Acids Res* 25:3389–3402. <https://doi.org/10.1093/nar/25.17.3389>.
60. Kimata N, Nishino T, Suzuki S, Kogure K. 2004. *Pseudomonas aeruginosa* isolated from marine environments in Tokyo Bay. *Microb Ecol* 47:41–47. <https://doi.org/10.1007/s00248-003-1032-9>.
61. Makino K, Oshima K, Kurokawa K, Yokoyama K, Uda T, Tagomori K, Iijima Y, Najima M, Nakano M, Yamashita A, Kubota Y, Kimura S, Yasunaga T, Honda T, Shinagawa H, Hattori M, Iida T. 2003. Genome sequence of *Vibrio parahaemolyticus*: a pathogenic mechanism distinct from that of *V. cholerae*. *Lancet* 361:743–749. [https://doi.org/10.1016/S0140-6736\(03\)12659-1](https://doi.org/10.1016/S0140-6736(03)12659-1).
62. Kondo H, Tinwongger S, Proespraiwong P, Mavichak R, Unajak S, Nozaki R, Hirano I. 2014. Draft genome sequences of six strains of *Vibrio parahaemolyticus* isolated from early mortality syndrome/acute hepatopancreatic necrosis disease shrimp in Thailand. *Genome Announc* 2(2): e00221-14. <https://doi.org/10.1128/genomeA.00221-14>.
63. Yang YT, Chen IT, Lee CT, Chen CY, Lin SS, Hor LI, Tseng TC, Huang YT, Sritunyalucksana K, Thitamadee S, Wang HC, Lo CF. 2014. Draft genome sequences of four strains of *Vibrio parahaemolyticus*, three of which cause early mortality syndrome/acute hepatopancreatic necrosis disease in shrimp in China and Thailand. *Genome Announc* 2(5):e00816-14. <https://doi.org/10.1128/genomeA.00816-14>.
64. Gomez-Jimenez S, Noriega-Orozco L, Sotelo-Mundo RR, Cantu-Robles VA, Cobian-Guemes AG, Cota-Verdugo RG, Gamez-Alejo LA, Del Pozo-Yauner L, Guevara-Hernandez E, Garcia-Orozco KD, Lopez-Zavala AA, Ochoa-Leyva A. 2014. High-quality draft genomes of two *Vibrio parahaemolyticus* strains aid in understanding acute hepatopancreatic necrosis disease of cultured shrimps in Mexico. *Genome Announc* 2(4):e00800-14. <https://doi.org/10.1128/genomeA.00800-14>.
65. Tang KF, Lightner DV. 2014. Homologues of insecticidal toxin complex genes within a genomic island in the marine bacterium *Vibrio parahaemolyticus*. *FEMS Microbiol Lett* 361:34–42. <https://doi.org/10.1111/1574-6968.12609>.